Biochemical and Biophysical Research Communications 618 (2022) 24–29

Contents lists available at ScienceDirect

Biochemical and Biophysical Research Communications

journal homepage: www.elsevier.com/locate/ybbrc

Cytosolic glutaredoxin 1 is upregulated in AMD and controls retinal pigment epithelial cells proliferation via β-catenin

Eva-Maria Hanschmann [a, b], Christina Wilms [a], Lisa Falk [b], Mariana Inés Holubiec [c], Stefan Mennel [d], Christopher Horst Lillig [b], José Rodrigo Godoy [e, *]

[a] Department of Neurology, Medical Faculty, Heinrich-Heine University, Düsseldorf, Germany
[b] Institute for Medical Biochemistry and Molecular Biology, University Medicine, University of Greifswald, Germany
[c] Instituto de Biología Celular y Neurociencia, Facultad de Medicina, Universidad de Buenos Aires, Argentina
[d] Hospital Feldkirch, Feldkirch, Austria
[e] Department of Veterinary Biomedical Sciences, College of Veterinary Medicine, Long Island University, NY, USA

ARTICLE INFO

Article history:
Received 12 May 2022
Received in revised form
1 June 2022
Accepted 8 June 2022
Available online 9 June 2022

Keywords:
Age-related macular degeneration
Glutaredoxin
ARPE-19
Hypoxia
β-catenin

ABSTRACT

Thioredoxin (Trx) family proteins are key players in redox signaling. Here, we have analyzed glutaredoxin (Grx) 1 and Grx2 in age-related macular degeneration (AMD) and in retinal pigment epithelial (ARPE-19) cells. We hypothesized that these redoxins regulate cellular functions and signaling circuits such as cell proliferation, Wnt signaling and VEGF release that have been correlated to the pathophysiology of AMD. ARPE-19 cells were transfected with specific siRNAs to silence the expression of Grx1 and Grx2 and were analyzed for proliferation/viability, migration capacity, β-catenin activation, and VEGF release. An active site-mutated C-X-X-S Grx1 was utilized to trap interacting proteins present in ARPE-19 cell extracts. In both, AMD retinas and in ARPE-19 cells incubated under hypoxia/reoxygenation conditions, Grx1 showed an increased nuclear localization. Grx1-silenced ARPE-19 cells showed a significantly reduced proliferation and migration rate. Our trapping approach showed that Grx1 interacts with β-catenin in a dithiol-disulfide exchange reaction. Knock-down of Grx1 led to a reduction in both total and active β-catenin levels. These findings add redox control to the regulatory mechanisms of β-catenin signaling in the retinal pigment epithelium and open the door to novel therapeutic approaches in AMD that is currently treated with VEGF-inhibitors.

1. Introduction

Age-related macular degeneration (AMD) constitutes the most common cause of severe, irreversible visual impairment in developed countries in the elderly [1]. Neovascular AMD, the “wet form”, is a rapid progressing disease [2]. The release of vascular endothelial growth factor (VEGF) by retinal pigmented epithelial (RPE) cells has been recognized as a key event in neovascular AMD. VEGF promotes the formation of new blood vessels from the choroid that invade the subretinal space [2–4] but the exact cause of its release remains elusive. Increased activity of β-catenin has been reported to induce the transcription of genes involved in cell proliferation and neovascularization such as VEGF [5,6] and an association between Wnt/β-catenin signaling and AMD has been established [7,8]. The accumulation of reactive oxygen species (ROS) in the RPE has also been considered a contributing factor to AMD [9,10]. Oxidoreductases of the thioredoxin family such as glutaredoxins (Grxs) are essential to maintain redox homeostasis and signaling [10–12]. These proteins are characterized by the presence of redox active cysteine residues within their active site that are crucial for their function in reducing protein disulfides (dithiol mechanism) and de-/glutathionylation reactions (monothiol mechanism) [13,14]. The glutaredoxin system is composed of Grxs, GSH and the NADPH-dependent GSH reductase [15]. Mammalian cells contain four Grxs located in the cytosol (Grx1 and Grx3) and mitochondria (Grx2 and Grx5) [16,17]. These proteins are abundantly expressed in ocular tissues [18,19] where they have been shown to confer protection to RPE cells (Grx1) [20] as well as to lens cells (Grx2) [21] exposed to hydrogen peroxide. Because AMD is associated with accumulation of oxidized biomolecules, tissue hypoxia, and enhanced RPE

* Corresponding author. Department of Veterinary Biomedical Sciences, College of Veterinary Medicine, Long Island University, 720 Northern Boulevard, Brookville, NY, 11548, USA.
E-mail address: Jose.Godoy@liu.edu (J.R. Godoy).

https://doi.org/10.1016/j.bbrc.2022.06.030

proliferation, we analyzed the cellular localization and function of Grx1 and Grx2 in ARPE-19 cells cultured under different oxygen conditions. Here, we show a key role of Grx1 in ARPE-19 cell proliferation and provide evidence for an involvement of Grx1 in β-catenin signaling, which is closely linked to AMD.

2. Material and methods

2.1. Immunohistochemistry and tissues

Human eyes (two AMD and two control) were derived from the Ophthalmological Clinic of the Philipps University Marburg's tissue bank and their use was in accordance with the Declaration of Helsinki for research involving material from human origin. AMD lesions were consistent with end-stage wet macular degeneration. Tissue sections were processed for immunohistochemistry as previously described [18] (see Supplementary Table S1 for primary antibody dilutions). Sections were analyzed with a Leica Diaplan microscope (Heidelberg, Germany) equipped with a MicroPublisher camera (QImaging, Surrey, BC, Canada). White balance was adjusted using the GNU image manipulation project software (www.gimp.org) and panels were arranged using Inkscape (www.inkscape.org). No additional image editing was performed.

2.2. Cell culture and hypoxia

Cells were cultivated in 1:1 DMEM (standard glucose concentration, 3.151 g/l; PAA, Pasching Austria) and Häms F12 medium (PAA, Pasching Austria) supplemented with 10% heat-inactivated fetal calf serum, 100 U/ml penicillin and streptomycin at 37 °C in a 90% humidified atmosphere containing 5% CO_2. Phenotype of ARPE-19 cells was assessed morphologically as well as by RT-PCR analysis of the RPE cell markers RPE65 and Best1 (see Supplementary Fig. S1). Cells were grown under different oxygen concentrations using a hypoxia chamber (Innova, New Brunswick) as follows: normoxic conditions, 20% O_2 for 24–48 h; hypoxia, 1% O_2 for 24 h; hypoxia/reoxygenation, 24 h 1% O_2 followed by 20% O_2 for 24 h. ARPE-19 cells were transiently transfected with 15 μg specific, custom-made siRNA (Eurogentech) (see Supplementary Table S2). Cells (3.5 million) were resuspended in electroporation buffer (21 mM HEPES, 137 mM NaCl, 5 mM KCl, 0.7 mM Na_2HPO_4, 6 mM D-glucose, pH 7.15), mixed with siRNA and electroporated in a total volume of 550 μl at 250 V, 1500 μF and 500 Ω. After adding FCS, cells were seeded out in conditioned medium (relation old to fresh medium 1:4). To increase knock-down efficiency, cells were transfected a second time after three days. Knock-down efficiency was analyzed by Western Blot (Grx1) and quantitative RT-PCR (Grx2).

2.3. Western blot

Cell extracts (20–40 μg of total protein) were mixed with sample loading buffer and reduced using 100 mM DTT. Proteins were separated by SDS-PAGE (Biorad) and blotted. Detection was conducted with specific primary antibodies (see Table S1 for dilutions) and a) a horseradish peroxidase secondary antibody and the ECL method or b) IR680 and IR800 secondary antibodies (Thermofisher) and near infrared fluorescence. Images were either obtained using a) the ChemiDoc™ XRS + System (Biorad) that allows to quantify total protein in each lane of a blot based on the stain-free technology, or b) the Odyssey infrared scanner (Li-Cor).

2.4. Quantitative and RT-PCR

RNA was isolated using the NucleoSpin RNA II kit (Macherey-Nagel, Germany). First strand cDNA was prepared using the RevertAid First Strand cDNA Synthesis Kit using 1 μg RNA as template and Oligo dT_{18} primer (Thermoscientific). Quantitative PCR (qPCR) was performed in the CFX96 Real Time System (Biorad) as a gradient from 55 °C to 65 °C using 1 μl cDNA, SensiMix SYBR HI-ROX containing SYBR Green I dye, dNTPs, stabilizers, a hot-start DNA polymerase (Bioline, London, UK) and specific primer against Grx2 (5′-CTGGTTTGGAGCAGGAGCGGCTC; 3′-GCCTATGAGTGTCAGTTGCACC) and GAPDH (5′-CAAGGTCATCCATGACAACTTTG; 3′- GTCCACCACCCTGTTGCTGTAG) as a reference in the ΔΔ Cq mode. The Biorad software was used for data analysis.

2.5. Immunofluorescence

ARPE-19 cells were fixed with 4% paraformaldehyde for 20 min at RT, and permeabilized and blocked (0.3% Triton X-100, 3% (w/v) BSA, 10 mM HEPES in PBS) for 1 h at room temperature. Primary antibody incubation was conducted overnight at 4 °C (see Supplementary Table S2 for dilutions). After washing, cells were incubated with Alexa-488 or 633 labelled secondary antibody (1:500 and 1:300, both Invitrogen) for 1 h at RT. F-actin was stained using phalloidin (Invitrogen), nuclei with 100 ng/ml DAPI (Sigma), and mitochondria using mitotracker (Invitrogen), according to manufacturer's recommendations. Coverslips were mounted with Mowiol and analyzed by fluorescence microscopy using a Leica TCS SP2 confocal laser scanning microscope (Leica, Heidelberg, Germany). Deconvolution was performed using the software package Huygens (Scientific Volume Imaging, Hilversum, The Netherlands).

2.6. Cell proliferation analysis

After the second transfection, 30,000–50,000 cells per well were seeded in a 96 well plate and cultured under different oxygen conditions as mentioned in section 2.2. Cell proliferation and viability was determined using the tetrazolium colorimetric assay according to the manufacturer's recommendations (MTT, Roth). Absorbance was measured at 550 nm in a Tecan plate reader (Maennedorf, Switzerland) against a blank without any cells. Cell proliferation was also assessed by BrdU incorporation. 20,000 ARPE-19-cells were seeded per well (24-well plate) and incubated overnight under normoxia or hypoxia/reoxygenation as described above. The next day, 10 μM BrdU were applied for 3 h at 37 °C. Afterwards cells were fixated with 4% PFA for 15 min before being exposed to 2 M HCl for 30 min at 37 °C. Cells were subsequently washed once with saturated tetraborate solution and twice with PBS containing 1% Triton-X 100. Unspecific binding sites were blocked using blocking buffer (5% normal goat serum, 0.2% Triton-X 100 in PBS) for 1 h. Anti-H4 (Merck) and anti-BrdU (Sigma-Aldrich) antibodies were diluted (1:1000 both) and mixed 1:1 in blocking buffer and PBS. Incubation occurred at 4 °C overnight. Cells were washed three times with PBS and incubated with secondary antibody cyanine dye conjugates (Millipore, 1:500 in blocking buffer) for 1 h at room temperature. Coverslips were removed from wells and mounted to an objective slide. For analysis, 5 randomly selected pictures per plate were made with the fluorescence microscope (BX51-Olympus) at 10× magnification. The number of BrdU positive cells was divided by the overall cell number indicated by H4 staining to determine the percentage of proliferating cells.

2.7. Scratch assay

150,000 ARPE-19-cells were seeded on fibronectin-coated glass slides. Cells were incubated overnight and the next day cells were kept at normoxia or were transferred to the hypoxic chamber for 24 h. The next day, a scratch with a 200 μl pipette tip was

performed according to Ref. [22]. Cells were cultured for additional 24 h and the cells and the gap size were documented at 0 h and 24 h following fixation with 4% PFA. For analysis, 2 pictures per scratch were taken with a fluorescence microscope (BX51-Olympus) at 4× magnification. The scratch width at two different points on each picture was determined using Image J (Rasband, USA). Scratch widths at 24 h were normalized to scratch width at 0 h for each condition (100%).

2.8. Intermediate trapping

The intermediate trapping approach was performed as described in Refs. [23,24]. Briefly, the C-terminal active site cysteine of human Grx1 was mutated to serine by site-directed mutagenesis using specific oligonucleotides (Fwd: ctgcccgtactccaggagggc, Rev: gccctcctggagtacgggcag). Grx1 in pet15b (Novagen, Darmstadt, Germany) was used as a template. The recombinant protein was expressed in *E. coli* as His-Tag fusion protein [18] and was purified using HisTrap columns according to the manufacturer's instructions (GE-Healthcare). For the trapping, 1 mg recombinant Cys-X-X-Ser protein re-buffered in PBS was loaded and reduced with 10 mM DTT on a His-Trap column. 10–20 mg ARPE19 cell lysate was added to the column. Disulfide-substrates were bound by the Grx1 mutant. Following thorough washing, substrates were eluted with 10 mM GSH. Proteins were precipitated with 20% TCA, washed with acetone and dissolved in urea-lysis buffer (6 M Urea, 50 mM Tris/HCl, 1% SDS) and were analyzed by Western Blotting.

2.9. ELISA and viability assay

Extracellular VEGF concentrations were analyzed using the VEGF Quantikine ELISA Kit from R&D systems (Minnesota, USA) according to the manufacturer's instructions. Supernatants were diluted (1:2–1:4) and VEGF concentrations were quantified using standards ($n = 6$) with known concentrations in the range of 0–1 pg/ml VEGF. VEGF levels in culture medium without cells were zero. Cell viability was assessed with the Cell Titer Blue (CTB) assay (Promega) according to the manufacturer's recommendations.

2.10. Software and statistical analysis

Western Blots were analyzed by Image Lab and Image J. Total protein in each lane of a blot was quantified based on the stain-free technology and the Image Lab software of Biorad and used for normalization of the blotting data obtained from densitometry analysis. Protein bands of the Western Blot were analyzed and quantified using the ImageJ software. Statistical analyses were conducted with GraphPad Prism 7. Results were expressed as mean ± SD. Significant differences in BrdU and scratch assay results were calculated using *t*-test. All other significant differences between groups were calculated with two-way ANOVA and Tukey's or Sidak's multi-comparison tests.

3. Results

3.1. Expression in AMD and changes in compartmentalization in ARPE-19

Both Grx1 and Grx2 showed increased immunoreactivities in the AMD retinas compared to those found in the controls (Fig. 1A). Strong Grx1 signals were detected in the nuclei of proliferating cells in AMD retinas (Fig. 1A). Nuclear Grx1 signals were especially evident in RPE cells that seemed less organized and hypertrophic in AMD patient 2 (arrows). In ARPE-19 cells cultured under hypoxia/reoxygenation, Grx1 showed stronger signals as compared to normoxic cells (Fig. 1B). Grx1 fluorescence was especially high in the nucleus. Grx2 showed a mitochondrial as well as a cytosolic localization.

3.2. Effects of Grx silencing on ARPE-19 cell viability

The knock-down efficiency for Grx2 was analyzed by qRT-PCR; the efficiency for Grx1 was analyzed by Western Blot (Fig. 2A and B). Cells transfected with control siRNA and cultivated under normoxia served as control and were set to 100%. Both Grx1 and Grx2 depleted cells showed significantly reduced viability scores compared with control cells. However, Grx1 depleted cells exhibited reductions in viability to less than 50% under hypoxia/reoxygenation compared with control and significantly lower than Grx2 depleted cells under the same conditions.

3.3. Effect of Grx1 silencing on cell proliferation and migration

Since Grx1 depletion resulted in the most significant reductions in cell viability, we focused our further experiments on this protein. Grx1 depletion led to a significant reduction of BrdU positive cells under normoxia (Fig. 3A and E) and hypoxia/reoxygenation conditions (Fig. 3B and F). The migration capacity of Grx1-depleted ARPE-19 cells was assessed in a scratch assay. Knocking down Grx1 significantly reduced cell migration under both normoxia (Fig. 3C and G) and hypoxia/reoxygenation conditions (Fig. 3D and H).

3.4. Grx1/β-catenin interaction, β-catenin expression and VEGF release

To further understand the mechanism by which Grx1 regulates ARPE-19 cells proliferation, we investigated β-catenin signaling, which is known to play an important role in AMD (Fig. 4). Our trapping experiment using a C-terminal active site mutated Grx1 (Cys-X-X-Ser) revealed the presence of β-catenin in the eluate as confirmed by Western blotting (Fig. 4A). Interestingly, only total β-catenin-detecting antibody provided a signal, whereas active β-catenin signal was absent. In addition to this, total β-catenin levels were increased in control cells under hypoxia/reoxygenation, whereas they remained unchanged in siGrx1 transfected cells under the same conditions (Fig. 4B and C). Corroboratively, active β-catenin levels were significantly reduced in siGrx1 transfected cells under hypoxia/reoxygenation conditions compared to control cells under the same conditions (Fig. 4D and E). Grx1 depleted cells showed a significantly reduced viability than control cells when cultured under normoxia or hypoxia/reoxygenation (Fig. 4F). VEGF release into the culture medium was significantly higher in siGrx1 cells under normoxia compared with control under the same conditions (Fig. 4G and H). Under hypoxia, VEGF release was still significantly higher in siGrx1 versus control cells. No differences between siGrx1 and control were observed under hypoxia/reoxygenation. However, VEGF levels of siGrx1 cells were significantly lower than those in siGrx1 cells under normoxic conditions (Fig. 4G).

4. Discussion

The understanding of mechanisms that regulate RPE function and proliferation is essential for the development of new therapeutic approaches for AMD. In this study, we report upregulation of Grx1 and Grx2 in AMD retinas, show nuclear translocation of Grx1 in ARPE-19 cells treated with hypoxia/reoxygenation, and reveal a role of Grx1 in RPE cell proliferation, potentially via the regulation of β-catenin. Thiol oxidoreductases in retinal cells may confer

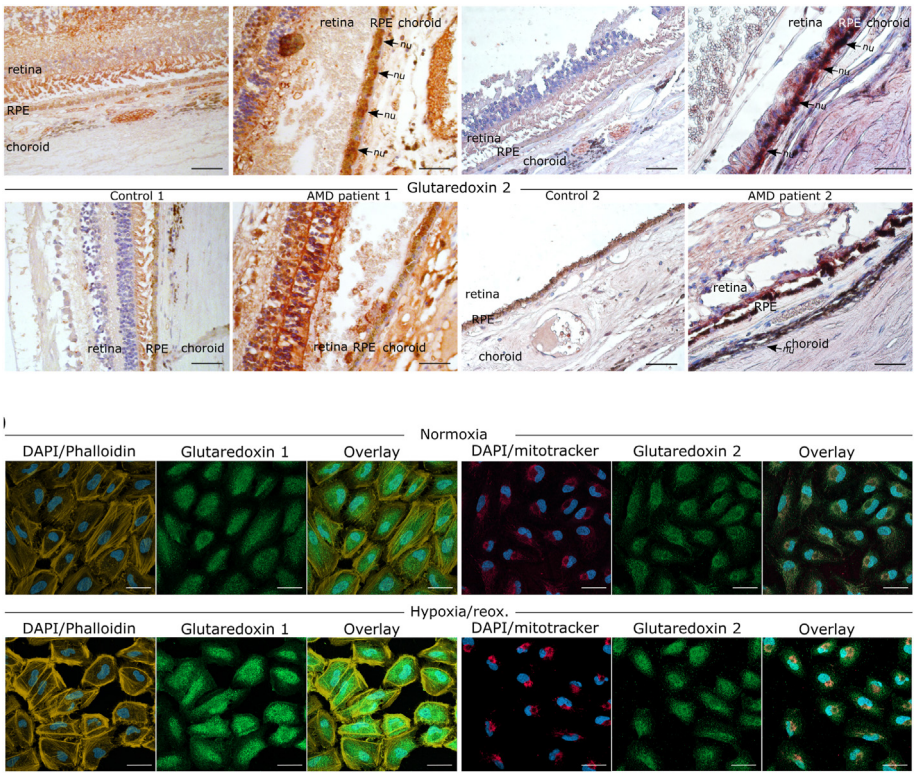

Fig. 1. (A) Distribution of redox proteins in of patients with and without age-related macular degeneration (AMD and control, respectively). Arrows indicate strong staining for Grx1 in the nuclei (nu) of retinal pigmented epithelial cells. Objective's magnification: 40×, scale bar: 50 μm. RPE, retinal pigmented epithelium. (B) Localization of Grx1 and 2 in ARPE-19 cells and changes in compartmentalization following hypoxia/reoxygenation. Objective's magnification: 100×, scale bar: 20 μm.

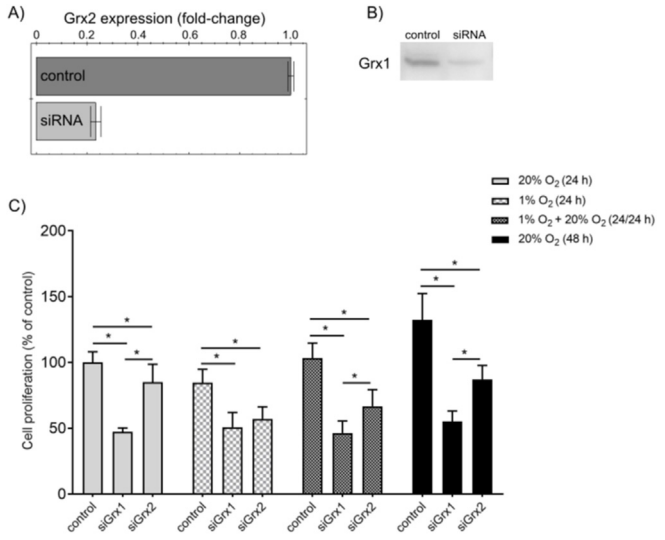

Fig. 2. Viability of ARPE-19 cells transfected with specific siRNAs. Knock-down efficiency verified by quantitative real time PCR (Grx2) (A) and Western blot analysis (Grx1). (B) Cell proliferation rate under different oxygen conditions (C). Columns represent mean ± SD (n = 30) of four independent experiments. Asterisks over columns show statistical significance ($P < 0.001$).

protection against cellular damage as it has been shown in mice exposed to white light [25] as well as in retinal epithelial cells exposed to chemicals such as hydrogen peroxide [20,26]. The reported role of hypoxia in the pathogenesis of AMD [4], prompted us to establish a hypoxia/reoxygenation model in ARPE-19 cells, which were phenotypically characterized by RPE-markers expression (Supplementary Fig. S1) and the formation of a cobblestone growth pattern (data not shown). ARPE-19 cells lacking Grx1 or Grx2 showed a significant reduction of cell proliferation. The most critical reduction in cell proliferation was obtained in cells lacking Grx1 and under hypoxia/reoxygenation conditions. Hence, we focused our research on understanding the mechanistic role of Grx1 in ARPE-19 cells proliferation.

Traditionally, studies analyzing protective functions of Grx1 have mostly focused on its cytosolic localization. Here, we show that Grx1 translocates to the cell nucleus in AMD patients as well as in ARPE-19 cells exposed to hypoxia/reoxygenation, and that Grx1 may be involved in the proliferation and migration of ARPE-19 cells. Anti-proliferative effects after silencing the expression of Grx1 were reported in primary human RPE cells exposed to 100 μM H_2O_2 [20]. Survival of RPE cells in the latter study was associated with Grx1-mediated deglutathionylation and activation of AKT—a kinase necessary for β-catenin phosphorylation and its nuclear translocation [27]. In our study, we provide evidence for a novel level of β-catenin regulation in ARPE-19 cells, i.e. dithiol-disulfide exchange. In the absence of Grx1, not only activation of β-catenin was dysregulated but also the overall levels of β-catenin were significantly reduced, compared with the control. Using the intermediate trapping approach, we confirmed Grx1/β-catenin interaction in ARPE-19 cells. Because in its reaction Grx1 forms an intermolecular disulfide with the interaction partners using the N-terminal cysteine [13], we suggest a thiol switch within β-catenin that may affect its ability to be phosphorylated by GSK-3 and subsequently ubiquitinated and degraded by the proteasome. Activation and nuclear translocation of β-catenin by a thioredoxin domain-containing protein (TXNDC12) has been shown in hepatocellular carcinoma cells [28]. Based on our *in vivo* and *in vitro* observations, Grx1 translocation into the cell nucleus occurs under

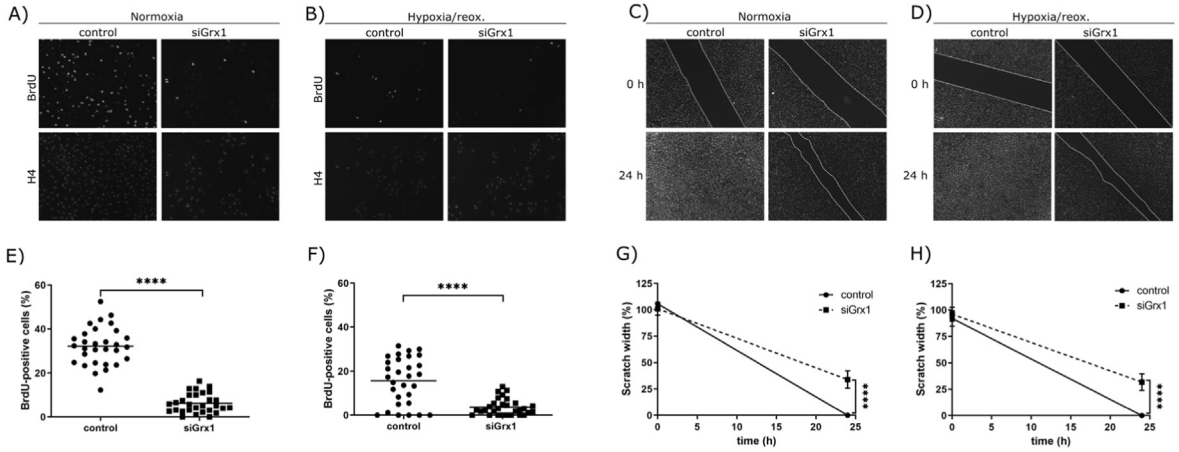

Fig. 3. Effect of Grx1 knockdown on ARPE-19 cells proliferation and migration. Representative pictures of control and siGrx1 transfected cells under normoxia (A) and hypoxia/reoxygenation (B). Scatter plots show percentage of BrdU positive cells over H4 positive ones on each field analyzed per treatment group (n = 30) (E, F). Line on each dataset represents the mean. Representative pictures of control and siGrx1 ARPE-19 cells showing the gap at the start (0 h) and 24 h later. Cells under normoxia (C) and hypoxia/reoxygenation (D) are shown. Graphs (G and H) represent the means ± SD (n = 12 for each treatment group; three independent experiments). Asterisks show significant differences between groups (P < 0.001).

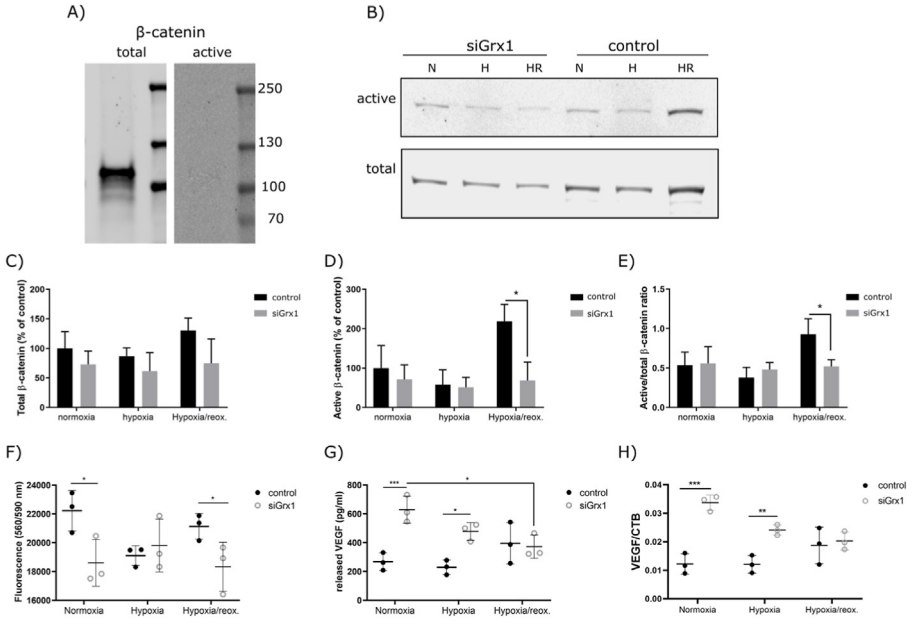

Fig. 4. Effect of Grx1 knock-down on β-catenin activity and VEGF release. (A) Detection of β-catenin by intermediate trapping. (B) Total and active β-catenin levels analyzed by Western blotting. (C–E) Densitometry analysis of Western blots. Columns represent mean ± SD of three independent experiments. Asterisks over columns show statistical significance (*P < 0.05). (F) Viability of ARPE-19 cells quantified by CTB assay. (G–H) VEGF levels quantified by ELISA. Columns represent mean ± SD of three independent experiments. N, normoxia (20% O_2 for 24 h); H, hypoxia (1% O_2 for 24 h); HR, hypoxia/reoxygenation (1% O_2 for 24 h followed by 20% O_2 for 24 h). Asterisks over columns show statistical significance (*P < 0.05, **P < 0.005, ***P < 0.001).

conditions of oxidative distress, such as hypoxia/reoxygenation. In the cell nucleus, thioredoxin family proteins were demonstrated to induce transcription factors activity such as NFkB via reduction of critical cysteine residues [29,30]. It is tempting to speculate that a redox interaction between Grx1/β-catenin in the cell nucleus might occur under hypoxia/reoxygenation conditions inducing the transcription of target genes. This might also be relevant for physiological signal transduction. One of the genes under β-catenin control is VEGF, which has been recognized as a key player in the progression of neovascular AMD. Current treatment of AMD includes anti-VEGF therapy in order to reduce cell proliferation and neovascularization. In our study, ARPE-19 cells lacking Grx1 produced significantly higher amounts of VEGF when cultured under normoxic and hypoxic conditions. However, this effect was not observed under hypoxia/reoxygenation conditions, where Grx1 depleted cells released significantly less VEGF than under normoxic conditions. These experiments need to be validated in the future using for instance primary RPE cells and longer and/or intermittent periods of hypoxia/reoxygenation.

In conclusion, Grx1 regulates ARPE-19 cell proliferation and represents a promising therapeutic target in AMD.

Declaration of competing interest

The authors declare that there is no conflict of interest regarding this paper.

Acknowledgements

The authors gratefully acknowledge the financial support by the Deutsche Forschungsgemeinschaft (SPP1710 – Dynamics of thiol-based redox switches in cellular physiology, Ha 8334/2-2, Li984/3-1, Li984/3-2, Li984/4-1) and the Research Office of Long Island University's College of Veterinary Medicine.

Appendix A. Supplementary data

Supplementary data to this article can be found online at https://doi.org/10.1016/j.bbrc.2022.06.030.

References

[1] H.R. Coleman, C.-C. Chan, F.L. Ferris, E.Y. Chew, Age-related macular degeneration, Lancet Lond. Engl. 372 (2008) 1835–1845, https://doi.org/10.1016/S0140-6736(08)61759-6.
[2] K. Kinnunen, G. Petrovski, M.C. Moe, A. Berta, K. Kaarniranta, Molecular mechanisms of retinal pigment epithelium damage and development of age-related macular degeneration, Acta Ophthalmol. (Copenh.) 90 (2012) 299–309, https://doi.org/10.1111/j.1755-3768.2011.02179.x.
[3] I. Bhutto, G. Lutty, Understanding age-related macular degeneration (AMD): relationships between the photoreceptor/retinal pigment epithelium/Bruch's membrane/choriocapillaris complex, Mol. Aspect. Med. 33 (2012) 295–317, https://doi.org/10.1016/j.mam.2012.04.005.
[4] M. Barben, M. Samardzija, C. Grimm, The role of hypoxia, hypoxia-inducible factor (HIF), and VEGF in retinal angiomatous proliferation, Adv. Exp. Med. Biol. 1074 (2018) 177–183, https://doi.org/10.1007/978-3-319-75402-4_22.
[5] J.J. Olsen, S.Ö.-G. Pohl, A. Deshmukh, M. Visweswaran, N.C. Ward, F. Arfuso, M. Agostino, A. Dharmarajan, The role of Wnt signalling in angiogenesis, Clin. Biochem. Rev. 38 (2017) 131–142.
[6] C.-M. Yang, S. Ji, Y. Li, L.-Y. Fu, T. Jiang, F.-D. Meng, β-Catenin promotes cell proliferation, migration, and invasion but induces apoptosis in renal cell carcinoma, OncoTargets Ther. 10 (2017) 711–724, https://doi.org/10.2147/OTT.S117933.
[7] J.B. Lin, A. Sene, L.A. Wiley, A. Santeford, E. Nudleman, R. Nakamura, J.B. Lin, H.V. Moolani, R.S. Apte, WNT7A/B promote choroidal neovascularization, Exp. Eye Res. 174 (2018) 107–112, https://doi.org/10.1016/j.exer.2018.05.033.
[8] Z. Lu, V. Lin, A. May, B. Che, X. Xiao, D.H. Shaw, F. Su, Z. Wang, H. Du, P.X. Shaw, HTRA1 synergizes with oxidized phospholipids in promoting inflammation and macrophage infiltration essential for ocular VEGF expression, PLoS One 14 (2019), https://doi.org/10.1371/journal.pone.0216808.
[9] S.G. Jarrett, M.E. Boulton, Consequences of oxidative stress in age-related macular degeneration, Mol. Aspect. Med. 33 (2012) 399–417, https://doi.org/10.1016/j.mam.2012.03.009.
[10] S. Beatty, H. Koh, M. Phil, D. Henson, M. Boulton, The role of oxidative stress in the pathogenesis of age-related macular degeneration, Surv. Ophthalmol. 45 (2000) 115–134.
[11] M.R. Liles, D.A. Newsome, P.D. Oliver, Antioxidant enzymes in the aging human retinal pigment epithelium, Arch. Ophthalmol. Chic. Ill 109 (1991) 1285–1288, https://doi.org/10.1001/archopht.1991.01080090111033, 1960.
[12] J. Cai, K.C. Nelson, M. Wu, P. Sternberg, D.P. Jones, Oxidative damage and protection of the RPE, Prog. Retin. Eye Res. 19 (2000) 205–221.
[13] E.-M. Hanschmann, J.R. Godoy, C. Berndt, C. Hudemann, C.H. Lillig, Thioredoxins, glutaredoxins, and peroxiredoxins–molecular mechanisms and health significance: from cofactors to antioxidants to redox signaling, Antioxidants Redox Signal. 19 (2013) 1539–1605, https://doi.org/10.1089/ars.2012.4599.
[14] C.H. Lillig, A. Holmgren, Thioredoxin and related molecules–from biology to health and disease, Antioxidants Redox Signal. 9 (2007) 25–47, https://doi.org/10.1089/ars.2007.9.25.
[15] A. Holmgren, C. Johansson, C. Berndt, M.E. Lönn, C. Hudemann, C.H. Lillig, Thiol redox control via thioredoxin and glutaredoxin systems, Biochem. Soc. Trans. 33 (2005) 1375–1377, https://doi.org/10.1042/BST20051375.
[16] E. Herrero, M.A. de la Torre-Ruiz, Monothiol glutaredoxins: a common domain for multiple functions, Cell. Mol. Life Sci. CMLS. 64 (2007) 1518–1530, https://doi.org/10.1007/s00018-007-6554-8.
[17] C.H. Lillig, C. Berndt, A. Holmgren, Glutaredoxin systems, Biochim. Biophys. Acta. 1780 (2008) 1304–1317, https://doi.org/10.1016/j.bbagen.2008.06.003.
[18] J.R. Godoy, M. Funke, W. Ackermann, P. Haunhorst, S. Oesteritz, F. Capani, H.-P. Elsässer, C.H. Lillig, Redox atlas of the mouse. Immunohistochemical detection of glutaredoxin-, peroxiredoxin-, and thioredoxin-family proteins in various tissues of the laboratory mouse, Biochim. Biophys. Acta 1810 (2011) 2–92, https://doi.org/10.1016/j.bbagen.2010.05.006.
[19] B. Upadhyaya, X. Tian, H. Wu, M.F. Lou, Expression and distribution of thiol-regulating enzyme glutaredoxin 2 (GRX2) in porcine ocular tissues, Exp. Eye Res. 130 (2015) 58–65, https://doi.org/10.1016/j.exer.2014.12.004.
[20] X. Liu, J. Jann, C. Xavier, H. Wu, Glutaredoxin 1 (Grx1) protects human retinal pigment epithelial cells from oxidative damage by preventing AKT glutathionylation, Invest. Ophthalmol. Vis. Sci. 56 (2015) 2821–2832, https://doi.org/10.1167/iovs.14-15876.
[21] H. Wu, K. Xing, M.F. Lou, Glutaredoxin 2 prevents H(2)O(2)-induced cell apoptosis by protecting complex I activity in the mitochondria, Biochim. Biophys. Acta 1797 (2010) 1705–1715, https://doi.org/10.1016/j.bbabio.2010.06.003.
[22] C.-C. Liang, A.Y. Park, J.-L. Guan, In vitro scratch assay: a convenient and inexpensive method for analysis of cell migration in vitro, Nat. Protoc. 2 (2007) 329–333, https://doi.org/10.1038/nprot.2007.30.
[23] L.D. Schütte, S. Baumeister, B. Weis, C. Hudemann, E.-M. Hanschmann, C.H. Lillig, Identification of potential protein dithiol-disulfide substrates of mammalian Grx2, Biochim. Biophys. Acta 1830 (2013) 4999–5005, https://doi.org/10.1016/j.bbagen.2013.07.009.
[24] C. Urbainsky, R. Nölker, M. Imber, A. Lübken, J. Mostertz, F. Hochgräfe, J.R. Godoy, E.-M. Hanschmann, C.H. Lillig, Nucleoredoxin-dependent targets and processes in neuronal cells, Oxid. Med. Cell. Longev. 2018 (2018), 4829872, https://doi.org/10.1155/2018/4829872.
[25] M. Tanito, H. Masutani, Y.-C. Kim, M. Nishikawa, A. Ohira, J. Yodoi, Sulforaphane induces thioredoxin through the antioxidant-responsive element and attenuates retinal light damage in mice, Invest. Ophthalmol. Vis. Sci. 46 (2005) 979–987, https://doi.org/10.1167/iovs.04-1120.
[26] E. Sugano, H. Isago, N. Murayama, M. Tamai, H. Tomita, Different anti-oxidant effects of thioredoxin 1 and thioredoxin 2 in retinal epithelial cells, Cell Struct. Funct. 38 (2013) 81–88.
[27] D. Fang, D. Hawke, Y. Zheng, Y. Xia, J. Meisenhelder, H. Nika, G.B. Mills, R. Kobayashi, T. Hunter, Z. Lu, Phosphorylation of beta-catenin by AKT promotes beta-catenin transcriptional activity, J. Biol. Chem. 282 (2007) 11221–11229, https://doi.org/10.1074/jbc.M611871200.
[28] K. Yuan, K. Xie, T. Lan, L. Xu, X. Chen, X. Li, M. Liao, J. Li, J. Huang, Y. Zeng, H. Wu, TXNDC12 promotes EMT and metastasis of hepatocellular carcinoma cells via activation of β-catenin, Cell Death Differ. (2019), https://doi.org/10.1038/s41418-019-0421-7.
[29] M. Lukosz, S. Jakob, N. Büchner, T.-C. Zschauer, J. Altschmied, J. Haendeler, Nuclear redox signaling, Antioxidants Redox Signal. 12 (2010) 713–742, https://doi.org/10.1089/ars.2009.2609.
[30] D. Daily, A. Vlamis-Gardikas, D. Offen, L. Mittelman, E. Melamed, A. Holmgren, A. Barzilai, Glutaredoxin protects cerebellar granule neurons from dopamine-induced apoptosis by activating NF-kappa B via Ref-1, J. Biol. Chem. 276 (2001) 1335–1344, https://doi.org/10.1074/jbc.M008121200.